European Radiology (2018) 28:3710–3718
https://doi.org/10.1007/s00330-018-5355-9

ONCOLOGY

In vivo study of enhanced chemotherapy combined with ultrasound image-guided focused ultrasound (USgFUS) treatment for pancreatic cancer in a xenograft mouse model

Eun-Joo Park[1,2] · Yun Deok Ahn[2] · Jae Young Lee[1,3]

Received: 13 July 2017 / Revised: 3 January 2018 / Accepted: 25 January 2018 / Published online: 29 March 2018

Abstract

Objectives This study was designed to investigate whether focused ultrasound (FUS) treatment with a higher mechanical index (MI) can enhance the effects of combined chemotherapy more than with a lower MI, and to evaluate the feasibility of the chemotherapy combined with FUS at a higher MI as an alternative treatment protocol.

Methods Mice in the first study were divided into six groups: control, chemotherapy only (GEM), two groups treated with FUS only at two different MIs, and two groups treated with chemotherapy and FUS (GEM + FUS). Mice were treated with a single-session treatment; one session consisted of three weekly treatments and 1 week of follow-up monitoring. In the second study, mice were assigned to two groups (GEM, GEM + FUS) and treated with four treatment sessions.

Results In the single-session treatment, tumor growth was most effectively suppressed in GEM + FUS group with a higher MI. Tumor growth rate was significantly lower in GEM + FUS group than in GEM group for multiple-session treatment. Specifically, three of ten mice in GEM + FUS group showed complete remission.

Conclusions This study demonstrated that FUS at a higher MI can enhance chemotherapy outcomes more than at a lower MI and demonstrated the potential of FUS in combination with chemotherapy as a new cancer treatment protocol.

Key points

- *Combined treatment of chemotherapy and focused ultrasound can effectively suppress tumor growth.*
- *For the focused ultrasound treatment conditions used in this study, focused ultrasound with relatively higher mechanical index shows more enhanced therapeutic outcomes than with the lower mechanical index.*
- *Combination therapy shows the possibility as a new cancer treatment protocol.*

Keywords Pancreatic cancer · Focused ultrasound · Chemotherapy · Mechanical index · Image guided

Abbreviations

BBB	blood–brain barrier
CR	complete response
FUS	focused ultrasound
GEM	gemcitabine
H&E	haematoxylin and eosin
IP	intraperitoneal
MI	mechanical index
USgFUS	ultrasound image-guided focused ultrasound

✉ Jae Young Lee
leejy4u@snu.ac.kr

[1] Biomedical Research Institute, Seoul National University Hospital, Seoul, Korea

[2] Department of Radiology, Seoul National University Hospital, Korea, Seoul, Korea

[3] Department of Radiology, Seoul National University College of Medicine, 101 Daehak-ro, Jongno-gu, Seoul 03080, Korea

Introduction

According to a report by the American Cancer Society, pancreatic cancer is the seventh most common cause of cancer-related deaths worldwide [1]. It has a relatively low rate of new cases compared to other common cancers, such as lung, breast and colorectal cancers. However, the incidence of pancreatic cancer has continuously increased, and it is usually fatal after it has been diagnosed [1, 2]. The 5-year survival rate of pancreatic cancer patients is less than 10%, and this rate has hardly been improved in the last 10 years [3]. Only 20% of

patients can be treated through surgery [4, 5]. While the treatment of inoperable pancreatic cancer patients primarily relies on chemotherapy or radiotherapy, these therapies have shown limited therapeutic effects [4]. Therefore, an alternative treatment protocol that can enhance the therapeutic effect of chemotherapy is required.

Several studies have shown promising results for focused ultrasound (FUS) cancer treatment, either by itself or in combination with traditional therapies [6–12]. FUS can produce diverse biological effects in tissue through either thermal or mechanical (non-thermal) means [13–17]. These bioeffects can therapeutically act on diseased tissue. FUS, by itself, can ablate cancerous tissue by rapidly elevating temperatures, as the result of accumulated acoustic energy [17, 18]. It can also physically remove cancer cells through the mechanical effects of FUS on tissue [19, 20]. The thermal and mechanical effects of FUS are also used for targeted drug delivery. It can temporarily open or create pathways in biological barriers so that more therapeutic agents can be delivered to the treatment site.

Cell membranes often limit chemotherapeutic agents from entering cells. Many researchers have studied how to improve the treatment outcomes of chemotherapy by developing disease-specific drugs or combining some methods that enhance cell membrane permeability [21–26]. As one of the enhancing methods, FUS can increase drug delivery rate to the cell interior [17, 27–29]. Stable cavitation activated by FUS can induce reversible and moderate cellular changes and temporarily create pores in the cell membrane that allow drugs to enter the cell. This effect, known as sonoporation, can be precisely induced in the body. Drug delivery enhanced by sonoporation can effectively be used in treating dense stroma, such as pancreatic cancers, with less systemic toxicity than traditional chemotherapy [30–32].

Our previous studies have shown that therapeutic outcomes of chemotherapy combined with FUS are enhanced at the lower acoustic energy level than the one used for thermal ablation [31, 33]. The results indicated that tumor growth was more effectively controlled by the combined treatment of chemotherapeutic agents with FUS and microbubbles. On the basis of previous study results and the fact that microbubbles can enhance the mechanical effects of FUS, a hypothesis was proposed that FUS treatment at a different mechanical index (MI) with the same total acoustic energy might result in different therapeutic effects on tumor growth. Therefore, this study was designed to investigate whether the therapeutic effects of the combined treatment of FUS and chemotherapy are enhanced by increasing the mechanical effects induced by FUS in targeted tissue. Two FUS treatment conditions at different MIs were used for this purpose. Additionally, we examined the feasibility of using FUS in combination with chemotherapy for pancreatic cancer patients using similar chemo-treatment protocols currently used in clinical practice.

Materials and methods

All animal experiments were performed according to the procedure approved by our Institutional Animal Care Use Committee (IACUC No. 15-0242). BALB/c male nude mice (Orientbio, Sungnamsi, Republic of Korea) weighing 25–35 g (6 weeks old) were used for the xenograft model. The animals were anaesthetized during all procedures with an intraperitoneal (IP) injection of zolazepam hydrochloride (30 mg/kg, Zoletil®, Virbac, Carros, France) and xylazine hydrochloride (10 mg/kg, Rompun 2%, Bayer Korea, Republic of Korea).

Cancer cell and xenograft mouse model preparation

Human pancreatic cancer cells, CFPAC-1 (ATCC, Manassas, VA, USA), were cultured in Dulbecco's Modified Eagle's medium (Invitrogen, San Diego, CA, USA) containing 10% foetal bovine serum and 1% penicillin/streptomycin. For cancer cell implantation, the cells were suspended in the culture medium at a concentration of 1×10^7 cells/ml. While the animals were under anaesthesia, a total of 1×10^6 cells were inoculated under the skin of the right flank in each mouse. Three weeks after the inoculation, the tumor size in each mouse was measured through ultrasound imaging prior to the treatments.

FUS treatment

All FUS treatments were performed using a preclinical FUS system (VIFU 2000®, Alpinion Medical Systems, Republic of Korea; Fig. 1a). The system has three transducer compartments: one for therapy, one for image guidance and one for size monitoring. The therapeutic transducer was composed of a single and spherical piezoelectric element, with 1.1 MHz resonance frequency. There was a circular opening measuring 40 mm in diameter at the centre for an imaging transducer. A linear array transducer (L8-17, 8–17 MHz), which was placed at the centre of the therapeutic transducer, was used for image guidance. Additionally, a phase array transducer (S12-4, 4–12 MHz) and an imaging module system (E-CUBE9®) were included for tumor volume monitoring.

Tumor-bearing animals were placed on an animal holder that was attached to a motorized 3D positioning system. Under the guidance of ultrasound images, the animal was positioned to locate the target tumor at the focus of therapeutic ultrasound. During the FUS treatment, noticeable motion was not observed in the real-time US images. All sonications were performed in a tank filled with degassed water (< 4 ppm) at 36 °C while the animal was submerged in the tank. According to the treatment plan of the system, the treatment target point was

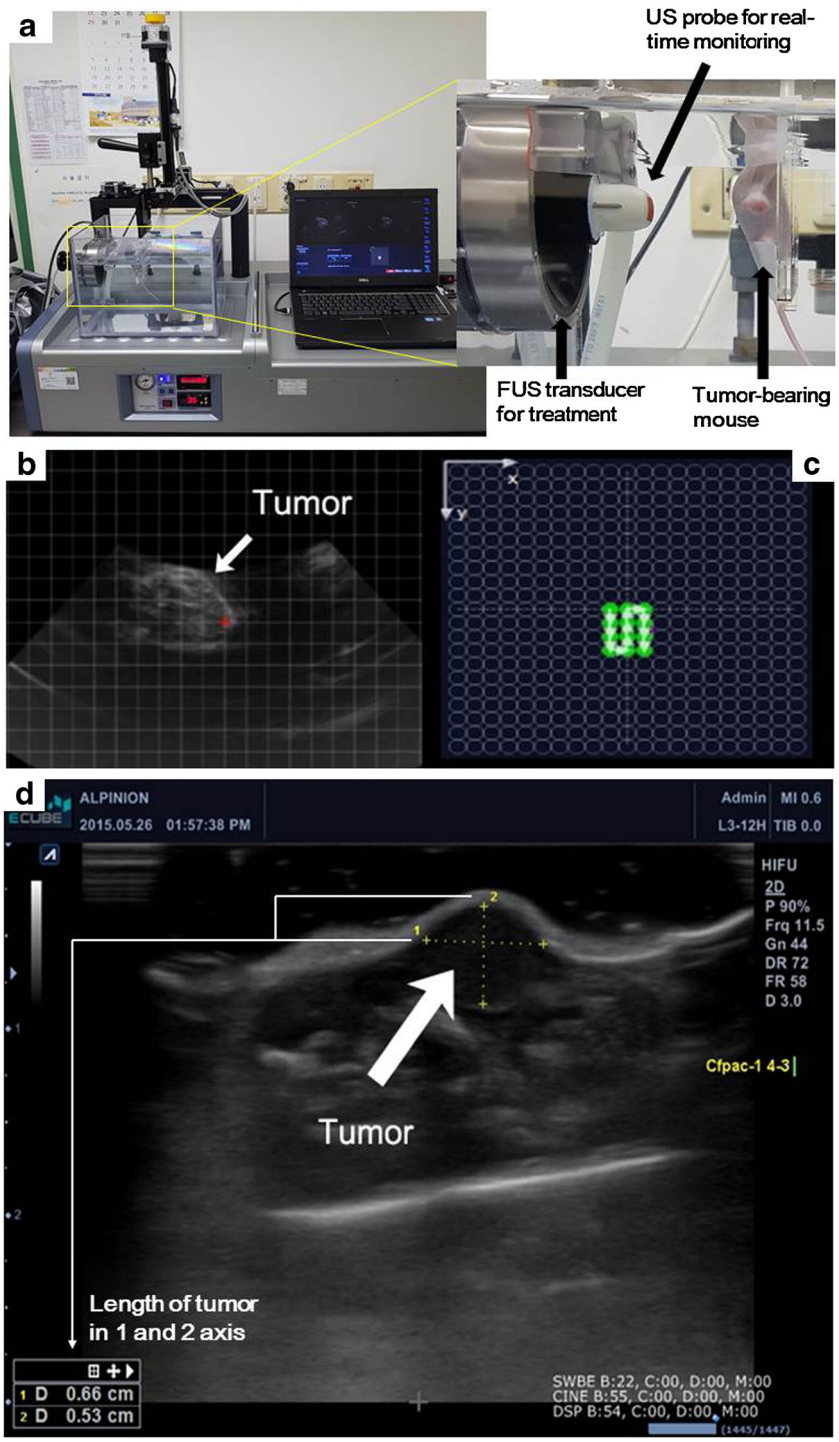

Fig. 1 The preclinical focused ultrasound system. a The FUS system has a transducer for therapy along with imaging transducer for image guidance. The tumor-bearing animal was placed on the animal holder. b Under ultrasound image guidance, the targeted tumor was located at the focus of therapy transducer. c The animal holder was precisely controlled in 3D and the FUS treatment was performed to cover the entire tumor with 2 mm between each sonication spot. d Ultrasound image of a tumor taken by a phase array transducer. To determine the tumor volume, an ultrasound image was taken every week during the experiments. The tumor volume was obtained by measuring the size in each axis from the image (yellow dotted line)

automatically moved 2 mm after each treatment (Fig. 1b, c). Each target point was sonicated for 20 s. The first FUS operating condition (FUS1) was determined by our previous study [31]. To evaluate the mechanical effects of ultrasound, the second operating condition (FUS2) was determined to have a higher MI, with total acoustic energy almost the same as the first FUS condition (FUS1). Details of the FUS operating parameters are listed in the Table 1.

Study design

The animal study was designed for two sub-studies: a single-session treatment study to investigate therapeutic effect of FUS according to the operating conditions and to determine the FUS protocol for the second sub-study, and a multiple-session treatment study to examine the clinical possibility of using FUS combined with chemotherapy.

Table 1 Operating conditions of FUS

Parameters	FUS1	FUS2
Acoustic power (W)	7.5	80.5
Acoustic energy (W s or J)	75	80.5
Peak negative pressure (MPa)	3.4	9.6
Mechanical index (MI)	3.2	9.2
Duty cycle (%)	50	5
PRF (Hz)	40	
Exposure time (s)	20	

* PRF: Pulse repetition frequency

Single-session treatment study

A total of 20 animals were randomly divided into six groups based on the treatment protocol: no treatment (control/n = 3), FUS treatment only at two different conditions (FUS1, lower MI/n = 3; FUS2, higher MI/n = 3), chemotherapy only (gemcitabine, GEM/n = 3) and combined treatment of chemotherapy with FUS treatment (GEM + FUS1/n = 4, GEM + FUS2/n = 4).

All animals, except those in the control group, were treated once a week for three consecutive weeks similar to the treatment protocol in the clinic. As the chemotherapeutic agent, gemcitabine (Gemzar®, Eli Lilly Co., Indianapolis, IN, USA) was administered through IP injection at a dose of 200 mg/kg. For the GEM + FUS groups, the animals were treated with FUS immediately after the gemcitabine injection, according to the protocol of our previous study [28]. Post-treatment monitoring for tumor growth was followed for 5 weeks.

Multiple session treatment study

A total of 20 animals were randomly divided into two groups: chemotherapy only (GEM) and combined chemotherapy with FUS treatment (GEM + FUS). The FUS condition for this study was determined by the results of single-session treatment study. Each treatment session consisted of three weekly treatments and 1-week follow-up monitoring (3 + 1) similar to the chemotherapy for pancreatic cancer in clinical practice. The animals were treated for a total of four treatment sessions. As in the single-treatment session study, gemcitabine was administered through IP injection, and the FUS treatment immediately followed in the GEM + FUS group. At the end of the study, tumor samples were collected for histologic evaluation.

Data analysis

Ultrasound images of tumor were obtained using the phase array transducer (S12-4, 4–12 MHz) weekly to determine the tumor volume. The volume was calculated by measuring the length of tumor in three axes from US images. The tumor size in each group was reported as the mean volume ± standard error. Histological analysis was performed through haematoxylin and eosin (H&E) staining to examine any differences between the treatments. Since it is assumed that each group has non-normal tumor volume distribution, the results were statistically analyzed using the Wilcoxon rank-sum test, and a p value less than 0.05 was considered to be significant.

Results

Single-session treatment

Tumor volume was obtained from the ultrasound images acquired weekly during the treatment and the follow-up monitoring (Fig. 2). The average initial tumor volume of all animals was 121.2 ± 5.3 mm^3, and the initial volumes in each group were not significantly different. The mean tumor volume of the control group and two FUS groups (FUS1 and FUS2) increased as a function of time from the beginning of the experiments. While the tumor growth of FUS1 was similar to that of the control group during the treatment (week 1–4) and post-treatment monitoring periods (week 5–8), the FUS2 group showed reduced tumor growth rate during the post-treatment monitoring period. Tumor growth in the GEM group was effectively suppressed during the treatment period, although it increased at week 6. During the treatment period, tumors in the groups treated with gemcitabine and FUS (GEM + FUS1 and GEM + FUS2) showed suppressed growth. In particular, the GEM + FUS2 group showed suppressed tumor growth up to week 6, which then started to increase at week 7. The tumor volume distributions of each group are plotted in Fig. 3 for the treatment and post-treatment periods. There were significant differences between the groups without GEM treatment (control, FUS1, FUS2) and the groups treated with GEM (GEM, GEM + FUS1, GEM + FUS2) ($p < 0.05$). During the treatment period, no significant volume difference was observed among the groups treated with gemcitabine (GEM, GEM + FUS1 and GEM + FUS2). However, there was a statistically significant volume difference between the GEM and GEM + FUS2 ($p < 0.05$) groups during the post-treatment monitoring period. Compared with other treatment conditions, treatment with GEM + FUS2 produced the most significant benefit. On the basis of these results, the GEM + FUS2 treatment was used in a multiple-session treatment study.

Multiple session treatment study

Figure 4 shows the tumor growth in each group for four treatment sessions. The arrows in Fig. 4 represent when the

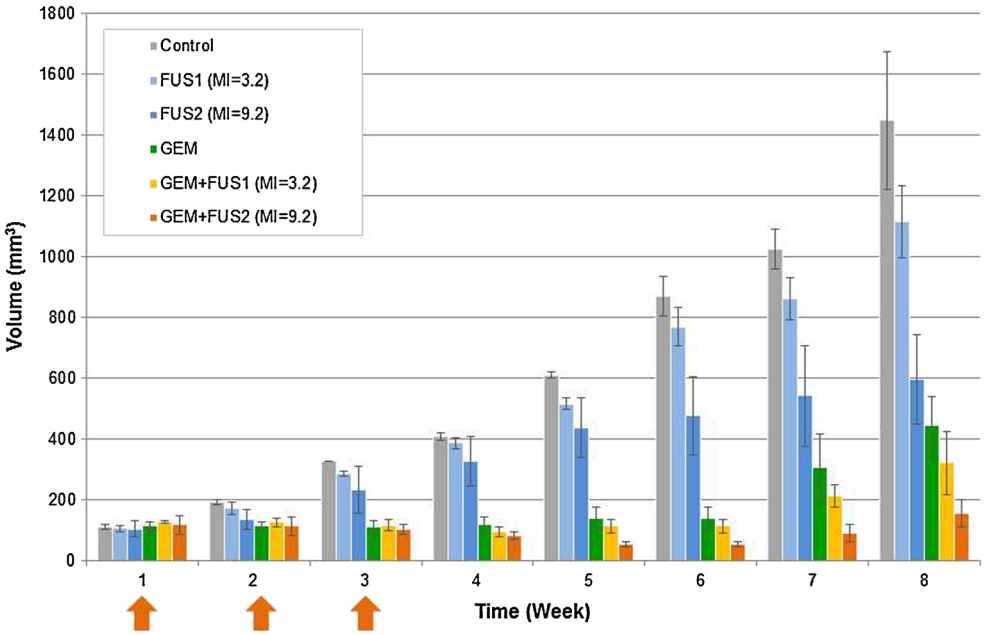

Fig. 2 Tumor volume of each group in the single-session treatment study. Arrows indicate three weekly treatments. Compared to the groups without gemcitabine treatment (control, FUS1, FUS2), the tumor volumes of the groups treated with gemcitabine either alone (GEM) or in combination with FUS (GEM + FUS1, GEM + FUS2) were effectively controlled. In particular, during the post-treatment period, the GEM + FUS2 group showed suppressed tumor growth that was significantly different from all other groups ($p < 0.05$)

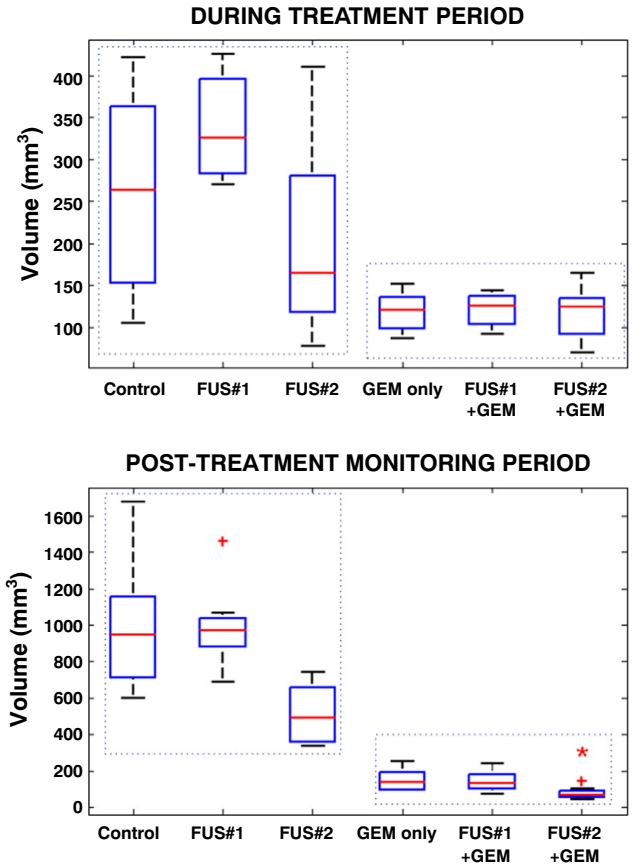

Fig. 3 Tumor volume distribution during the treatment (week 1–4) and post-treatment (week 5–8) periods. During the treatment period and post-treatment period, the tumor volumes of the groups without gemcitabine treatment (within dotted line) showed no significant therapeutic effects. Among the groups treated with gemcitabine (within solid line), the tumor volume of the GEM + FUS2 group showed a statistically significant difference during the post-treatment period (*$p < 0.05$)

weekly treatments were performed. For both treatment conditions, the tumor growth was effectively suppressed until the second treatment session (TS2 in Fig. 4). However, tumors in the group treated with gemcitabine alone grew extensively after the second treatment session. Well-suppressed tumors in the GEM + FUS group also grew, but the growth rate was much lower than that in the GEM group. For the third and fourth treatment sessions, the mean doubling time of the tumor volume was calculated using nonlinear least-squares regression. The doubling times were 14.0 ± 1.1 days and 22.8 ± 3.29 days for the GEM and GEM + FUS groups, respectively.

Tumor volume distributions for each treatment session are shown in Fig. 5. There was a statistically significant difference between the groups from the second treatment session ($p < 0.05$). With four GEM + FUS treatment sessions, three of the ten animals in the GEM + FUS group showed complete responses (CR, CR rate = 30%), while one of the ten animals in the GEM group showed CR (CR rate = 10%). Data from these CR cases are not included in Figs. 4 and 5. Even without the CR cases, the combined treatment of GEM and FUS showed significantly effective tumor control after the first treatment session ($p < 0.01$).

Histological examination using H&E staining was performed on representative samples from each group, as shown in Fig. 6. The treated areas of all CR cases in the GEM + FUS group (Fig. 6c) showed no trace of tumor. For non-CR cases, no significant histological changes such as obvious coagulative necrosis with surrounding congestion, haemorrhage or inflammatory cell infiltration were observed.

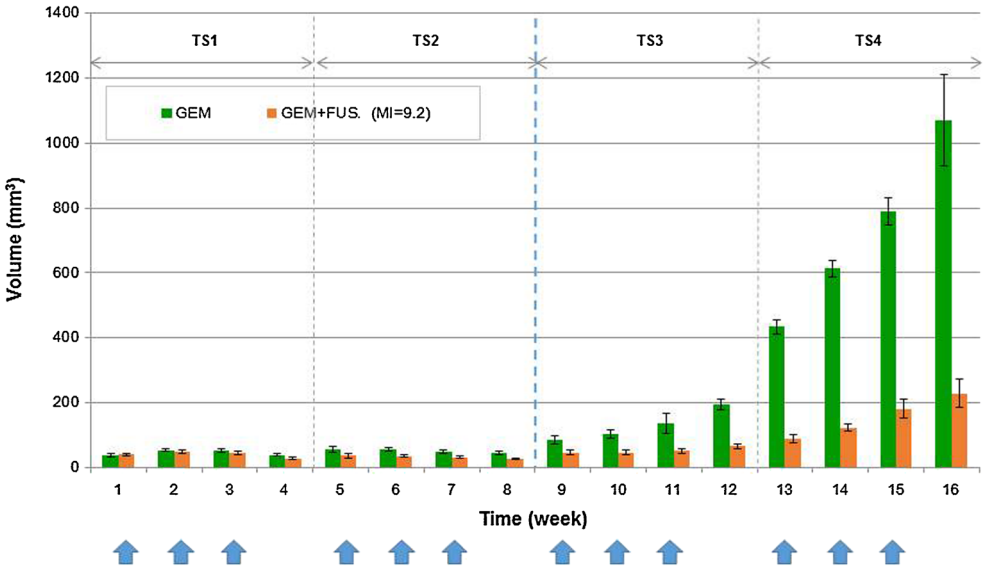

Fig. 4 Tumor volume of multiple-session treatment study. In both treatment groups, tumor growth was well suppressed until the second treatment session (TS2). However, fast tumor growth was observed in the GEM group from the third treatment session (TS3), while it was suppressed in the GEM + FUS group, indicating that the tumor might become resistant to gemcitabine. Arrows indicate the weekly treatment for each treatment session (TS)

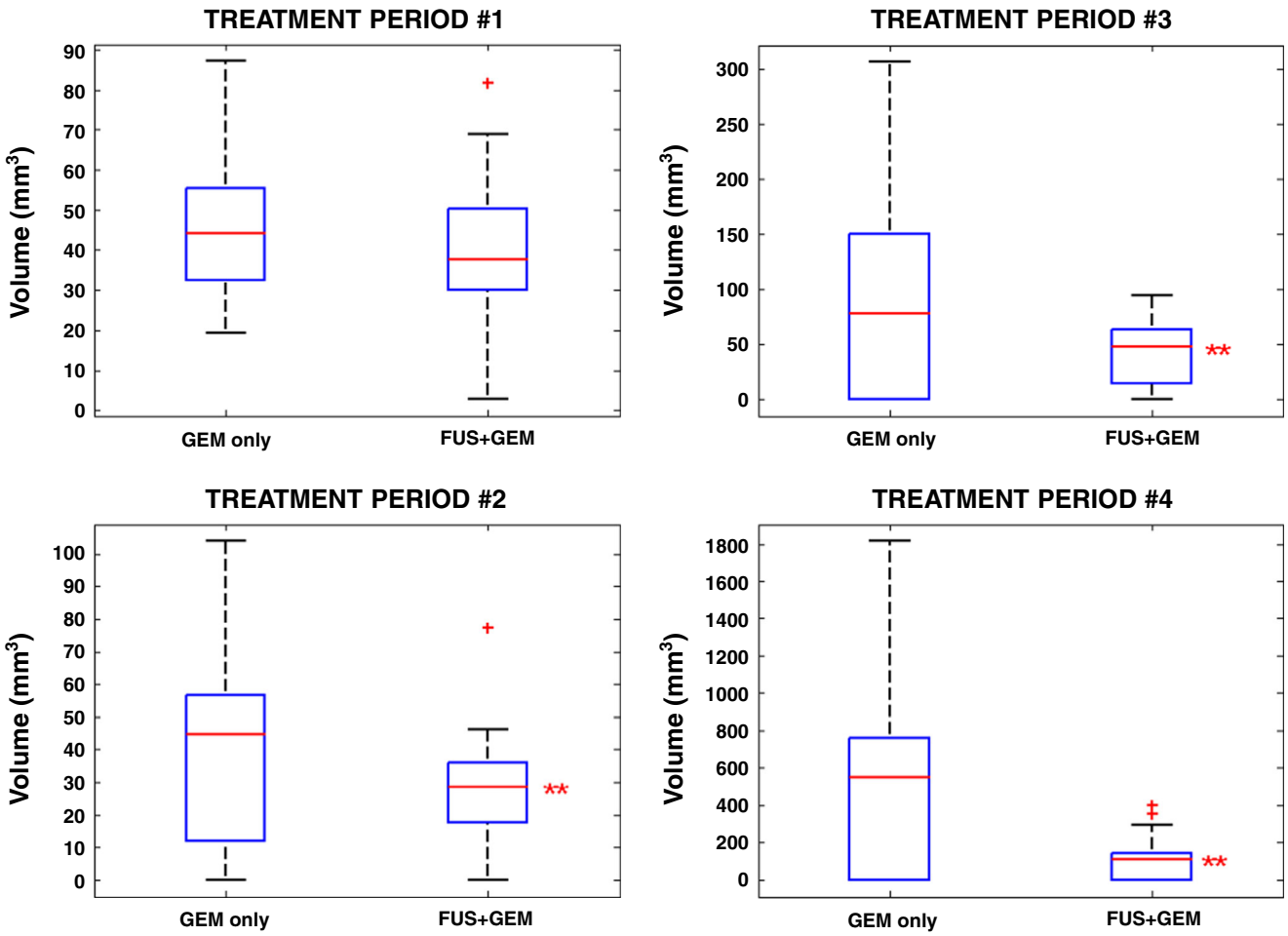

Fig. 5 Distribution of the tumor volume for each treatment session. From the second treatment session, a statistically significant difference in tumor volume distribution was observed between the groups (**$p < 0.01$)

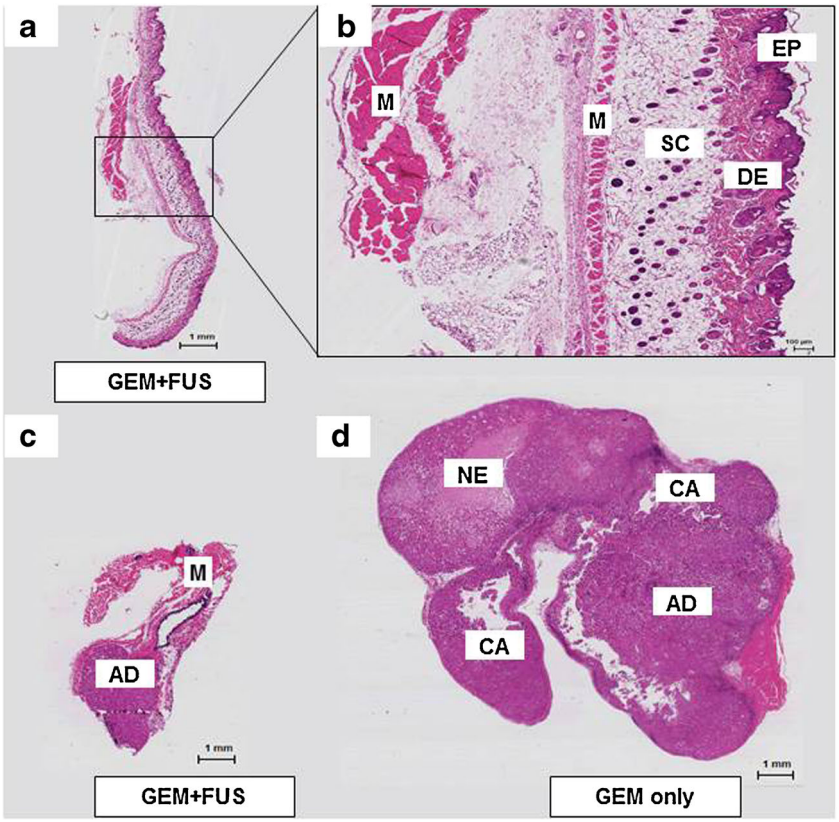

Fig. 6 Representative images of H&E-stained pancreatic cancer (CFPAC-1) cells. a (×40) and b (×100) are images from the GEM + FUS2 group after showing complete response. Histological images of tumors in the GEM + FUS2 group (c) and in the GEM group (d). Other than the tumor size, there was no significant histological difference between groups. EP epidermis, DE dermis, SC subcutaneous tissue, M muscle, AD adenocarcinoma, CA cystic degeneration, NE necrosis

Discussion

In medical applications, FUS has been widely investigated as a treatment tool either by itself or in combination with current therapies. Noninvasiveness and treatment localization are the advantages of FUS [34, 35]. FUS can be used in cancer surgery (thermal or non-thermal ablation), targeted drug delivery (BBB opening [12, 36, 37], sonoporation [38–40], transdermal delivery [41], mild hyperthermia [42]) and biological modulation (neuromodulation [43] and immunomodulation [44]). Thermal ablation through high intensity FUS is currently used in the clinic to treat uterine fibroids, prostate cancer, pain from bone metastasis, essential tremor and several other diseases [45]. Mechanical (non-thermal) effects of FUS have gained increased interest, and this study was designed on the basis of the mechanical effects of FUS for drug delivery.

The results of single-session treatment study showed that FUS enhanced the therapeutic effects of chemotherapeutic agents. Among the groups treated with FUS alone, a slightly higher effect was observed in the FUS2 group, which had an MI that was approximately three times higher than that of the FUS1 group, with almost the same amount of total acoustic energy at each treatment point, although the enhancement was small in the FUS-only groups. Tumor growth in the group treated with a combination of chemotherapeutic agents and FUS at a higher MI was more effectively suppressed compared to chemotherapy only and combined therapy at a lower MI. The results of the single-session treatment study indicate that FUS can increase the therapeutic effects of chemotherapy and that FUS with a higher MI might induce higher drug uptake by cancer cells. From these results, it can be assumed that the mechanical effects of FUS might be more effective in an FUS-mediated treatment.

A multiple-session treatment study was designed to mimic the treatment protocol that is currently used in clinical practice for pancreatic cancer. It involved repeating three weekly treatments and 1 week of monitoring. By repeating the treatment with chemotherapeutic agents alone, pancreatic cancer CFPAC-1 showed extremely reduced therapeutic effects after a couple of treatment sessions. It is believed that the cancer cells become drug resistant as the treatment is repeated. Compared to chemotherapeutic agents alone, the combined treatment of chemotherapeutic agents and FUS showed significantly slower tumor growth as the treatment session was repeated. In particular, three of the ten animals in the combined treatment group showed CR (CR rate = 30%), while one of the ten animals showed CR (CR rate = 10%) in the chemotherapeutic agent-only group. With the enhanced CR rate of combined treatment, these results demonstrated the possibility of FUS treatment combined with chemotherapy as an alternative treatment protocol for pancreatic cancer care.

In several studies of therapeutic effects of focused ultrasound, researchers have used microbubbles to enhance the therapeutic effects of FUS [37, 46–50]. The studies have

shown that the enhanced treatment outcomes are mainly through the mechanical effects of FUS.

The results presented herein demonstrate that FUS at a higher MI enhances cancer treatment. However, the effects of microbubbles in combined therapy at different MI of FUS were not investigated in this study. Therefore, chemotherapy combined with microbubble-enhanced FUS treatment at a higher MI should be further investigated to determine the mechanism of FUS at a higher MI in combined therapy.

As a basic study, our study demonstrates the feasibility of combined treatment protocol of chemotherapy and FUS as a potential treatment protocol. However, the following limitations have to be overcome to move the protocol toward clinical use. The heterotopic xenograft model used in this study has a limited ability to represent the actual conditions of pancreatic cancer in clinical practice. While this study shows that the mechanical effects induced by FUS play an important role in enhancing the therapeutic outcomes, any possible mechanisms of FUS in combined therapy have not been investigated. To move this treatment protocol toward clinical applications, the main mechanism of FUS in combined therapy with chemotherapeutic agent should be investigated by accurately monitoring any cavitational activities and temperature changes that might be induced by FUS.

Funding This study has received funding by the National Research Foundation of Korea, which is funded by the Ministry of Science, ICT & Future Planning (2012R1A1A1010930).

Compliance with ethical standards

Guarantor The scientific guarantor of this publication is Jae Young Lee.

Conflict of interest The authors of this manuscript declare no relationships with any companies whose products or services may be related to the subject matter of the article.

Statistics and biometry No complex statistical methods were necessary for this paper.

Basic statistical methods were used by the authors who are well trained in clinical statistics.

Informed consent This study was performed on animal models.

Ethical approval Approval from the institutional animal care committee of Seoul National University Hospital was obtained.

Methodology
- prospective
- experimental
- performed at one institution.

References

1. American Cancer Society (2011) Global cancer facts & figures, 2nd edn. American Cancer Society, Atlanta. https://www.cancer.org/content/dam/cancer-org/research/cancer-facts-and-statistics/global-cancer-facts-and-figures/global-cancer-facts-and-figures-2nd-edition.pdf. Accessed 12 Jun 2017
2. Ferlay J SI, Ervik M, Dikshit R, Eser S, Mathers C, Rebelo M, Parkin DM, Forman D, Bray F (2013) GLOBOCAN 2012 v1.0, cancer incidence and mortality worldwide. IARC CancerBase
3. The Surveillance, Epidemiology, and End Results (SEER) Program of the National Cancer Institute. SEER cancer facts: pancreas cancer. https://seer.cancer.gov/statfacts/html/pancreas.html. Accessed 22 Nov 2017
4. Kamisawa T, Wood LD, Itoi T, Takaori K (2016) Pancreatic cancer. Lancet 388:73–85
5. Amrutkar M, Gladhaug IP (2017) Pancreatic cancer chemoresistance to gemcitabine. Cancers 9:–157
6. de Senneville BD, Moonen C, Ries M (2016) MRI-guided HIFU methods for the ablation of liver and renal cancers. Adv Exp Med Biol 880:43–63
7. Peek MC, Ahmed M, Scudder J, Baker R, Pinder SE, Douek M (2016) High intensity focused ultrasound in the treatment of breast fibroadenomata: results of the HIFU-F trial. Int J Hyperthermia 32:881–888
8. Quinn SD, Gedroyc WM (2015) Thermal ablative treatment of uterine fibroids. Int J Hyperthermia 31:272–279
9. Zhao WP, Han ZY, Zhang J, Yu XL, Cheng ZG, Zhou X et al (2016) Early experience: high-intensity focused ultrasound treatment for intra-abdominal aggressive fibromatosis of failure in surgery. Br J Radiol 89:20151026
10. Hersh DS, Kim AJ, Winkles JA, Eisenberg HM, Woodworth GF, Frenkel V (2016) Emerging applications of therapeutic ultrasound in neuro-oncology: moving beyond tumor ablation. Neurosurgery 79:643–654
11. Lin Q, Mao KL, Tian FR, Yang JJ, Chen PP, Xu J et al (2016) Brain tumor-targeted delivery and therapy by focused ultrasound introduced doxorubicin-loaded cationic liposomes. Cancer Chemother Pharmacol 77:269–280
12. Park EJ, Zhang YZ, Vykhodtseva N, McDannold N (2012) Ultrasound-mediated blood-brain/blood-tumor barrier disruption improves outcomes with trastuzumab in a breast cancer brain metastasis model. J Control Release 163:277-284
13. Dalecki D (2004) Mechanical bioeffects of ultrasound. Ann Rev Biomed Eng 6:229-248
14. American Institute of Ultrasound in Medicine (2000) Section 6–mechanical bioeffects in the presence of gas-carrier ultrasound contrast agents. J Ultrasound Med 19:54–68
15. American Institute of Ultrasound in Medicine (2000) Section 5–nonthermal bioeffects in the absence of well-defined gas bodies. J Ultrasound Med 19, 54-68
16. Miller DL, Smith NB, Bailey MR, Czarnota GJ, Hynynen K, Makin IR (2012) Overview of therapeutic ultrasound applications and safety considerations. J Ultrasound Med 31:623–634
17. O'Brien WD Jr (2007) Ultrasound-biophysics mechanisms. Prog Biophys Mol Biol 93:212–255
18. Humphrey VF (2007) Ultrasound and matter–physical interactions. Prog Biophys Mol Biol 93:195–211
19. Hoogenboom M, Eikelenboom D, den Brok MH, Heerschap A, Futterer JJ, Adema GJ (2015) Mechanical high-intensity focused ultrasound destruction of soft tissue: working mechanisms and physiologic effects. Ultrasound Med Biol 41:1500–1517
20. Khokhlova VA, Fowlkes JB, Roberts WW, Schade GR, Xu Z, Khokhlova TD et al (2015) Histotripsy methods in mechanical

disintegration of tissue: towards clinical applications. Int J Hyperthermia 31:145–162
21. Cao Y, Gao M, Chen C, Fan A, Zhang J, Kong D et al (2015) Triggered-release polymeric conjugate micelles for on-demand intracellular drug delivery. Nanotechnology 26:115101
22. Karavelidis V, Bikiaris D, Avgoustakis K (2015) New thermosensitive nanoparticles prepared by biocompatible pegylated aliphatic polyester block copolymers for local cancer treatment. J Pharm Pharmacol 67:215–230
23. Ta T, Bartolak-Suki E, Park EJ, Karrobi K, McDannold NJ, Porter TM (2014) Localized delivery of doxorubicin in vivo from polymer-modified thermosensitive liposomes with MR-guided focused ultrasound-mediated heating. J Control Release 194:71-81
24. Wang A, Gao H, Sun Y, Sun YL, Yang YW, Wu G et al (2013) Temperature- and pH-responsive nanoparticles of biocompatible polyurethanes for doxorubicin delivery. Int J Pharm 441:30–39
25. Yu D, Li W, Zhang Y, Zhang B (2016) Anti-tumor efficiency of paclitaxel and DNA when co-delivered by pH responsive ligand modified nanocarriers for breast cancer treatment. Biomed Pharmacother 83:1428–1435
26. Sanson C, Diou O, Thevenot J, Ibarboure E, Soum A, Brulet A et al (2011) Doxorubicin loaded magnetic polymersomes: theranostic nanocarriers for MR imaging and magneto-chemotherapy. ACS Nano 5:1122–1140
27. Helfield B, Chen X, Watkins SC, Villanueva FS (2016) Biophysical insight into mechanisms of sonoporation. Proc Natl Acad Sci U S A 113:9983–9988
28. Shi D, Guo L, Duan S, Shang M, Meng D, Cheng L et al (2016) Influence of tumor cell lines derived from different tissue on sonoporation efficiency under ultrasound microbubble treatment. Ultrason Sonochem. https://doi.org/10.1016/j.ultsonch.2016.08.022
29. ter Haar G (2007) Therapeutic applications of ultrasound. Prog Biophys Mol Biol 93:111–129
30. Kotopoulis Kotopoulis S, Delalande A, Popa M, Mamaeva V, Dimcevski G, Gilja OH et al (2014) Sonoporation-enhanced chemotherapy significantly reduces primary tumor burden in an orthotopic pancreatic cancer xenograft. Mol Imaging Biol 16:53–62
31. Yu MH, Lee JY, Kim HR, Kim BR, Park EJ, Kim HS et al (2016) Therapeutic effects of microbubbles added to combined high-intensity focused ultrasound and chemotherapy in a pancreatic cancer xenograft model. Korean J Radiol 17:779–788
32. Kotopoulis S, Stigen E, Popa M, Safont MM, Healey A, Kvale S et al (2017) Sonoporation with Acoustic Cluster Therapy (ACT®) induces transient tumor volume reduction in a subcutaneous xenograft model of pancreatic ductal adenocarcinoma. J Control Release 245:70–80
33. Lee ES, Lee JY, Kim H, Choi Y, Park J, Han JK et al (2013) Pulsed high-intensity focused ultrasound enhances apoptosis of pancreatic cancer xenograft with gemcitabine. Ultrasound Med Biol 39:1991–2000
34. ab Ithel Davies I, Gavrilov LR, Tsirulnikov EM (1996) Application of focused ultrasound for research on pain. Pain 67:17–27
35. Yudina A, Moonen C (2012) Ultrasound-induced cell permeabilisation and hyperthermia: strategies for local delivery of compounds with intracellular mode of action. Int J Hyperthermia 28:311–319
36. Park J, Zhang Y, Vykhodtseva N, Akula JD, McDannold NJ (2012) Targeted and reversible blood-retinal barrier disruption via focused ultrasound and microbubbles. PloS one 7:e42754
37. Aryal M, Park J, Vykhodtseva N, Zhang YZ, McDannold N (2015) Enhancement in blood-tumor barrier permeability and delivery of liposomal doxorubicin using focused ultrasound and microbubbles: evaluation during tumor progression in a rat glioma model. Phys Med Biol 60:2511–2527
38. Okunaga S, Takasu A, Meshii N, Imai T, Hamada M, Iwai S et al (2015) Ultrasound as a method to enhance antitumor ability of oncolytic herpes simplex virus for head and neck cancer. Cancer Gene Ther 22:163–168
39. Qin J, Wang TY, Willmann JK (2016) Sonoporation: applications for cancer therapy. Adv Exp Med Biol 880:263–291
40. Jin Z, Choi Y, Ko SY, Park JO, Park S (2017) Experimental and simulation studies on focused ultrasound triggered drug delivery. Biotechnol Appl Biochem 64:134–142
41. Park EJ, Werner J, Smith NB (2007) Ultrasound mediated transdermal insulin delivery in pigs using a lightweight transducer. Pharm Res 24:1396–1401
42. Chae SY, Kim YS, Park MJ, Yang J, Park H, Namgung MS et al (2014) High-intensity focused ultrasound-induced, localized mild hyperthermia to enhance anti-cancer efficacy of systemic doxorubicin: an experimental study. Ultrasound Med Biol 40:1554–1563
43. Ventre DM, Koppes AN (2016) The body acoustic: ultrasonic neuromodulation for translational medicine. Cells Tissues Organs 202:23–41
44. Cohen-Inbar O, Xu Z, Sheehan JP (2016) Focused ultrasound-aided immunomodulation in glioblastoma multiforme: a therapeutic concept. J Ther Ultrasound 4:2
45. Focused Ultrasound Foundation. Disease and conditions. https://www.fusfoundation.org/diseases-and-conditions-all/overview. Accessed 12 Jun 2017
46. Coussios CC, Farny CH, Haar GT, Roy RA (2007) Role of acoustic cavitation in the delivery and monitoring of cancer treatment by high-intensity focused ultrasound (HIFU). Int J Hyperthermia 23:105–120
47. Kopechek JA, Park EJ, Zhang YZ, Vykhodtseva NI, Mcdannold NJ, Porter TM (2014) Cavitation-enhanced MR-guided focused ultrasound ablation of rabbit tumors in vivo using phase shift nanoemulsions. Phys Med Biol 59:3465–3481
48. Lammertink BH, Bos C, van der Wurff-Jacobs KM, Storm G, Moonen CT, Deckers R (2016) Increase of intracellular cisplatin levels and radiosensitization by ultrasound in combination with microbubbles. J Control Release 238:157–165
49. Tachibana K, Endo H, Feril LB, Nejad SM, Takahashi H, Narihira K et al (2015) Enhanced mechanical damage to in vitro cancer cells by high-intensity-focused ultrasound in the presence of microbubbles and titanium dioxide. J Med Ultrason (2001) 42:449–455
50. Liu HL, Fan CH, Ting CY, Yeh CK (2014) Combining microbubbles and ultrasound for drug delivery to brain tumors: current progress and overview. Theranostics 4:432–444